Self-produced hydrogen sulfide improves ethanol fermentation by *Saccharomyces cerevisiae* and other yeast species

Emilio Espinoza-Simón [1#], Paola Moreno-Alvarez [1#], Elias Nieto-Zaragoza [1], Carolina Ricardez-García [2], Emmanuel Ríos-Castro [3], Salvador Uribe-Carvajal [2] and Francisco Torres-Quiroz [1,*]

[1] División de Ciencia Básica, Departamento de Bioquímica y Biología Estructural, Instituto de Fisiología Celular, Universidad Nacional Autónoma de México (UNAM), Ciudad de México, México

[2] División de Ciencia Básica, Departamento de Genética Molecular, Instituto de Fisiología Celular, Universidad Nacional Autónoma de México (UNAM), Ciudad de México, México

[3] Unidad de Genómica, Proteómica y Metabolómica, LaNSE, Centro de Investigación y de Estudios Avanzados del I.P.N., Ciudad de México, México

These authors contributed equally to this work

***** Correspondence: ftq@ifc.unam.mx

Abstract

Hydrogen sulfide (H_2S) is a gas produced endogenously in organisms from the three domains of life. In mammals, it is involved in diverse physiological processes, including the regulation of blood pressure, and its effects on memory. In contrast, in unicellular organisms the physiological role of H_2S has not been studied in detail. In yeast, for example, in the winemaking industry H_2S is an undesirable byproduct because of its rotten egg smell; however, its biological

relevance during fermentation is not well understood. The effect of H_2S in cells is linked to a posttranslational modification in cysteine residues known as S-persulfidation. We evaluated S-persulfidation in the *Saccharomyces cerevisiae* proteome. We screened S-persulfidated proteins from cells growing in fermentable carbon sources and we identified several glycolytic enzymes as S-persulfidation targets. Pyruvate kinase, catalyzing the last irreversible step of glycolysis, increased its activity in the presence of a H_2S donor. Yeast cells treated with H_2S increased ethanol production; moreover, mutant cells that endogenously accumulated H_2S produced more ethanol and ATP during the exponential growth phase. This mechanism of the regulation of the metabolism seems to be evolutionarily conserved in other yeast species, because H_2S induces ethanol production in the pre-Whole Genome Duplication species *Kluyveromyces marxianus* and *Meyerozyma guilliermondii*. Our results suggest a new role of H_2S in the regulation of the metabolism during fermentation.

Keywords: H_2S; S-persulfidation; fermentation; yeast; metabolism; posttranslational modification; hydrogen sulfide.

Introduction

Hydrogen sulfide (H_2S) is a gasotransmitter produced endogenously in cells. It has been associated with diverse physiological processes such as vasodilation [1], pain [2] and longevity in animals [3], plant growth and development [4], bacterial antibiotic resistance [5], and as a byproduct of alcoholic fermentation in yeast [6]. Surprisingly, the biological function of H_2S in yeast is not fully understood [7]; the majority of reports describe how it is produced or how to prevent its production during fermentation [8–10]. In yeast, H_2S is involved in heavy metal detoxification [11], population synchrony [12], and chronological

aging [3]; however the molecular mechanisms behind these phenomena have not been fully elucidated.

In yeast, the main metabolic pathway that produces H_2S is the sulfate assimilation pathway [13], where inorganic sulfate is transformed to H_2S and used in the synthesis of methionine and cysteine. This pathway is highly active in the exponential growth phase, as the principal H_2S producer, sulfite reductase (encoded by *MET5* and *MET10*) [6], is highly active. The synthesis of H_2S takes place in the first hours of fermentation and decreases at the final stages when cells reach the stationary phase [14]. The sulfur transferase Tum1p is another protein involved in H_2S production during fermentation when high concentrations of cysteine are present in the media [15]. H_2S is metabolized by Met17p a sulfhydrylase that catalyze the incorporation of sulfide for the biosynthesis of sulfur-containing amino acids [16].

The molecular effect of hydrogen sulfide depends on a posttranslational modification named S-persulfidation (originally termed sulfhydration) [17]. S-persulfidation involves addition of a thiol group to the cysteine residues (-S-SH) in proteins. This posttranslational modification has been associated with the activation and inhibition of protein activity [17,18].

In this work, for the first time, we evaluated the S-persulfidation of yeast proteins. We report that hydrogen sulfide is a regulator of glycolysis that increases ethanol production in *S. cerevisiae*. This was observed using an exogenous donor of hydrogen sulfide or mutant strains that accumulate or produce less H_2S. This mechanism of regulation was conserved in pre-Whole Genome Duplication (WGD) species, such as the thermotolerant *Kluyveromyces marxianus* from the KLE clade and the oleaginous yeast *Meyerozyma guilliermondii* from the CUG-Ser1 clade. This work provides an insight into how H_2S regulates glucose metabolism through an evolutionarily conserved mechanism, constituting an important role of H_2S in fermentation.

Materials and Methods

Yeast strains, media, and growth conditions

Saccharomyces cerevisiae strains used in this study were S288C-derived laboratory strains BY4742 (*MATα his3Δ1 leu2Δ0 lys2Δ0 ura3Δ0*) referred as *wt*, BY4741 (*MATa his3Δ1 leu2Δ0 met17Δ0 ura3Δ0*). *Kluyveromyces marxianus* and *Meyerozyma guilliermondii* were isolated from mezcal producers in Michoacán, México [19]. Deletion strains derived from BY4742 were constructed by PCR-based gene replacement [20] using synthetic oligonucleotides and the kanMx and natMx disruption modules contained in plasmids pUG6 and pAG25. Gene deletions were confirmed by PCR using A and D oligos. Strains and oligonucleotides are listed in supplementary table 1. Strains were cultured at 30ºC in liquid YPD medium (1% yeast extract, 2% dextrose, 2% peptone) or YPG medium (1% yeast extract, 2% galactose, 2% peptone) until reaching the exponential growth phase (optical density at 660nm [OD660] =0.5-0.6) and cells were collected then for protein extraction.

Reagents

Sodium hydrosulfide (NaHS), Methyl methanethiosulfonate (MMTS), dithiothreitol (DTT), antibiotin antibody, neocuproine, deferoxamine and others chemicals were purchased from Sigma-Aldrich, St Louis MO, rabbit polyclonal anti-GAPDH (GTX100118, Genetex) were purchased from Genetex, Irvine, CA and N-(6-(biotinamido)hexyl)-3′-(2′-pyridyldithio)-propionamide (HPDP-biotin) (sc-207359), mouse monoclonal anti-enolase (sc-21738), goat polyclonal anti-CBS (sc-46830) and rabbit polyclonal anti-TIM (FL-249) were purchased from Santa Cruz Biotech, Dallas Tx.

106 *Modified biotin switch assay*

107 The modified biotin switch assay was performed as described previously [17,21].
108 Briefly, after yeast cultures reached exponential phase, cells were collected, and
109 intracellular proteins were extracted with chilled glass-beads in HEN buffer (250
110 mM HEPES-NaOH pH 7.7, 1 mM EDTA) supplemented with 1% triton X-100, 0.1
111 mM neocuproine, 0.1 mM deferoxamine and 1X protease cocktail inhibitor
112 (Roche, Switzerland). Cell lysates were centrifuged at 16900 x *g* for 1 hr at 4ºC,
113 total extracts (1-2 mg) were blocked in HEN buffer with 2.5% SDS and 20 mM
114 MMTS at 50ºC for 20 min. The MMTS was removed by acetone precipitation and
115 the protein pellet was resuspended in HEN buffer with 1% SDS. Protein labeling
116 was performed with 0.8 mM HPDP-biotin for 3 h at room temperature in the dark.
117 The biotinylated proteins were separated by SDS-polyacrylamide gel
118 electrophoresis (PAGE) and subjected to immunoblot analysis.

119

120 *Purification of biotinylated proteins*

121 After biotin switch assay, labeled extracts were subjected to streptavidin-based
122 affinity precipitation with magnetic beads. Labeled extracts were incubated with
123 3X volumes of neutralization buffer (20 mM HEPES-NaOH pH 7.7, 100 mM NaCl,
124 1 mM EDTA, 0.5% triton) and 25 µl of streptavidin magnetic beads (Pierce) with
125 agitation, overnight at 4ºC. Magnetic beads were collected and washed with wash
126 buffer as indicated by manufacturer's instructions, biotinylated proteins were
127 eluted with IP-MS elution buffer and analyzed using LS-MS or SDS-PAGE.

128

129 *Immunoblot analysis*

130 Protein extracts were separated by SDS-PAGE and transferred to polyvinylidene
131 difluoride (PVDF) membranes (Millipore-Merck, Germany). Membranes were

blocked with 5% non-fat milk and incubated with a specific anti-biotin antibody overnight at 4ºC. Proteins were detected with chemiluminescence using horse-radish peroxidase conjugated secondary antibodies (Jackson ImmunoResearch, West Grove, PA). Before to immunoblot, membranes were stained using Ponceau red (Millipore-Merck, Germany) as protein loading control.

Quantification of intracellular ATP concentration

NaHS was added to cells cultures at specific timepoints, then cells were centrifuged, and intracellular ATP was measured using the ATP Bioluminescent Assay Kit HS II (Roche, Switzerland). Cell samples were prepared by diluting treated cells to a final concentration of 3.7x109 cells·mL^{-1} in 500 µl with a buffer containing 100 mM Tris-HCl pH 7.8 and 4 mM EDTA. After 2 min incubation, samples were immersed in boiling water for 2 minutes, and the resulting cell extracts were incubated for 5 minutes at 4ºC, cell debris were removed by centrifugation at 16900 x *g* for 5 min and supernatants were used to measure the amount of intracellular ATP using an ATP calibration curve prepared each time, as indicated by the manufacturer. Bioluminescence was detected in a POLARstar Omega luminometer (BGM LABTECH, Offenburg, Germany). Three independent experiments with three replicas were performed, and values are represented as mean ± standard error.

Detection of H_2S production

H_2S production by yeast strains colonies was detected through the generation of a visible black precipitate indicating that the hydrogen sulfide gas has reacted with lead nitrate [22]. Yeast strains were diluted, and cell density normalized to 3x10^7 cells·mL^{-1}. Cells were spotted in solid media (3.2% dextrose, 0.4% yeast extract, 0.24% peptone, 0.016% ammonium sulfate, 0.08% lead nitrate, 1.6%

agar) and plates were kept at 30ºC for 5-7 days. Also, H_2S production was measured as reported previously [23] with some modifications. BY4742 *wt* strain were precultured at 30ºC with constant shaking for 2 days in fresh YPD media. The assay was performed on a 96 well plate (COSTAR). Each well had 185 µL of YPD media, 5 µL of methylene blue (1 mg·mL^{-1}) diluted in citrate buffer (100 mM, pH 4.5) and 10 µL of cells, for a final OD_{600} of 0.2. Growth was measured in an Infinite 200 (TECAN, Life Sciences) at 600 nm and 663 nm during 15 hours with intervals of 15 minutes between readings. During measures cells were incubated at 30ºC with occasionally shaking. Three experimental replicates were made, with six different biological replicates in each experiment. Data for the hydrogen sulfide production were analyzed with the following formula:

$$\frac{((OD_{600nm\ t0} - OD_{663nm\ t0}) - (OD_{600nm\ tx} - OD_{663nm\ tx})}{OD_{600nm\ tx}\ from\ no\ reaction\ mix}$$

Fermentation assays

BY4742 *wt* and derived mutants were precultured in liquid YPD medium for 24 h at 30ºC, under agitation at 90 rpm in an Excella E24 incubator Shaker (New Brunswick Scientific, USA), then were inoculated in a 2L flask containing 500 mL of fresh YPD with an initial OD_{600}=0.2 and incubated in the same conditions. When cells reached DO_{660}=0.5, a pulse of NaHS was added. After 7h of NaHS addition, aliquots of 2 ml were obtained, DO_{660} was measured, and cells centrifuged at 16900 x *g* for 1 min. Supernatants were stored at -20ºC for subsequent ethanol quantification. For mutant and *wt* strains, aliquots were taken every hour after cells were inoculated, supernatants were stored at -20ºC. Ethanol production was evaluated through enzymatic assay coupled to NAD^+ reduction. Briefly, supernatants were incubated in buffer (114 mM K_2HPO_4 pH 7.6), 1.8 mM NAD^+ and 39µg·mL^{-1} alcohol dehydrogenase (ADH) for 30 min at 30ºC with vigorous agitation [24]. Produced NADH was monitored by the increase in absorbance at 340 nm. The results are reported as mM ethanol per 1x10^7 cells.

Three independent experiments with three replicas were performed, and values are represented as mean ± standard error. *K. marxianus* fermentation assay was performed as in *S. cerevisiae* strains, when cells reached DO_{660}=0.5, a pulse of NaHS 0.1mM was added. After 7h of NaHS addition, aliquots of 2 ml were obtained, and ethanol was qunatified. For *Meyerozyma guilliermondii* when cells reached DO_{660}=0.5, a pulse of NaHS 0.1mM was added, 24h later another pulse of same concentration was added and 7h later ethanol was quantified.

Enzymes activity assays

Glyceraldehyde 3 phosphate dehydrogenase (GAPDH) [17], pyruvate kinase (PK) [25] and alcohol dehydrogenase (ADH) [26] activities were measured by specific reaction assays and monitored spectrophotometrically at 340 nm, recording the rate of NAD to NADH reduction. Cells cultures were exposed to NaHS at different times, protein extracts were quantified, and 10 µg of protein were incubated in assay buffer as follows: for GAPDH (20 mM Tris-HCl pH 7.8, 100 mM NaCl, 0.1 $mg \cdot mL^{-1}$ Bovine serum albumin, 2 mM NAD^+, 10 mM sodium pyrophosphate, 20 mM sodium arsenate, 500 mM DTT buffer, phosphate buffered saline (PBS) 1X, 27.3 mM glyceraldehyde 3-phosphate [G3P]). For PK (50 mM Imidazole·HCl, 120 mM KCl, 62 mM $MgSO_4$ pH 7.6, 45 mM ADP, 6.6 mM NADH, 45 mM phosphoenolpyruvate [PEP], 1.3 $KU \cdot mL^{-1}$ lactate dehydrogenase). For ADH (114 mM K_2HPO_4 pH 7.6), 1.8 mM NAD+, and 16.4 mM ethanol). Three independent experiments with three replicas were performed, and values are represented as mean ± standard error.

Oxygen consumption rate assay

BY4742 *wt* and derived mutant cells were precultured in liquid YPD medium for 48 hrs at 30°C, then were cultured in YPD medium with an initial DO_{600}=0.2 under

agitation in an Excella E24 incubator (New Brunswick Scientific, USA) for 7h at 30°C. Basal oxygen consumption was measured in resting cells with a Clark electrode (Oximeter model 782, Warner/Strathkelvin Instruments, North Lanarkshire, Scotland) in a water-jacketed chamber. Temperature was kept at 30 °C using a water bath (PolyScience 7 L, IL). Oxygen consumption reaction mixture was MES 10 mM pH 6 and 500 mg (wet weight) of cells were added at chamber [24]. To evaluate role of NaHS addition, when BY4742 cells reached OD_{600}=0.5, a pulse of 0.1 mM NaHS was added. Seven hours later, basal oxygen consumption was measured as abovementioned. Results are reported as natgO/wet weight g/ mn and values are represented as mean ± standard error. et weight) of cells were added at chamber.

Sample preparation and LC-MALDI-MS/MS

Biotinylated proteins were digested with 250 ng of trypsin mass spectrometry grade (Sigma-Aldrich, St. Louis, MO) in 50 mM of ammonium bicarbonate (ABC). Resulting tryptic peptides were desalted using ZipTip C18 (Millipore) and concentrated to an approximated volume of 10 µL. Afterward, 9 µL were loaded into ChromXP Trap Column C18-CL precolumn (Eksigent, Redwood City CA); 350 µm X 0.5 mm, 120 Aº pore size, 3 µm particle size and desalted with 0.1% trifluoroacetic acid (TFA) in H2O at a flow of 5 µL min^{-1} for 10 min. Then, peptides were loaded and separated on a 3C18-CL-120 column (Eksigent, Redwood City CA); 75 µm X 150 mm, 120 Aº pore size, 3 µm particle size, in a HPLC Ekspert nanoLC 425 (Eksigent, Redwood City CA) using as a mobile phase A, 0.1% TFA in H_2O and mobile phase B 0.1% TFA in acetonitrile (ACN) under the following lineal gradient: 0-3 min 10% B, 60 min 60% B, 61-64 min 90 % B, 65 to 90 min 10% B at a flow of 250 nL min^{-1}. Eluted fractions were automatically mixed with a solution of 2 $mg{\cdot}mL^{-1}$ of alfa-cyano-4-hydroxycinnamic acid (CHCA) in 0.1% TFA and 50% ACN as a matrix, spotted in an Opti-TOF plate of 384 spots using a MALDI Ekspot (Eksigent, Redwood City CA) with a spotting velocity of 20 s per spot at a matrix flow of 1.6 µL min^{-1}. The generated spots were analyzed by a

MALDI-TOF/TOF 4800 Plus mass spectrometer (ABSciex, Framingham MA). Each MS Spectrum was acquired by an accumulation of 1000 shots in a mass range of 850-4000 Th with a laser intensity of 3800. The 100 more intense ions with a minimum signal-noise (S/N) of 20 were programmed to fragmenting. The MS/MS spectra were obtained by fragmentation of selected precursor ions using Collision-Induced Dissociation (CID) and acquired by 3000 shots with a laser intensity of 4300. Generated MS/MS spectrums were compared using Protein Pilot software v. 2.0.1 (ABSciex, Framingham MA) against *Saccharomyces cerevisiae*, strain ATCC 204508/S288c database (downloaded from Uniprot, 6049 protein sequences) using Paragon algorithm. Search parameters were: Not constant modifications in cysteines, trypsin as a cutter enzyme, all the biological modifications and amino acids substitution set by the algorithm (including carbamidomethylated cysteine as a variable modification); as well as phosphorylation emphasis and Gel-based ID as special factors. The detection threshold was considered in 1.3 to acquire 95% of confidence; additionally, the identified proteins showed a local FDR of 5% or less. Since a peptide derived from a given fragmentation spectra may be shared among redundant proteins during database search, it is necessary group all competing proteins and report only the protein with more spectrometric evidence; for this reason, identified proteins were grouped by ProGroup algorithm contained in the software Protein Pilot to minimize redundancy.

Results

S-Persulfidation of yeast proteins growing on a fermentable carbon source

Protein S-persulfidation was detected using the modified biotin switch method [17]. In order to validate the method in yeast, we performed the assay in either a poor producer (*met5*Δ*met10*Δ) or an accumulator (*met17*Δ) strain of H_2S and compared them to the *wt* (BY4742) (Figure 1A). Cells were grown using glucose as the carbon source, and at the exponential phase, when H_2S is produced [6],

the protein was extracted. S-Persulfidated proteins were accumulated in *met17*Δ in comparison to the *met5*Δ*met10*Δ strain and wt as expected (Figure 1B).

In yeast, H_2S is produced during fermentation, however, the S-persulfidation target proteins are not known. We used mass spectrometry to analyze the S-persulfidated proteins in cells growing at the exponential phase in two different fermentable carbon sources: glucose and galactose. Glucose is the preferred fermentable carbon source of yeast, while galactose needs to be isomerized to enter the glycolytic pathway. We found 42 S-persulfidated proteins; 21 were specific to glucose-grown cells, 4 were specific to galactose-grown cells, and 17 proteins were found in both conditions (Supplementary Table 2). Among the generally expressed 17 proteins, 15 were reported before as proteins with a redox-regulated cysteine [27], which is a feature of cysteines susceptible to posttrans-lational modifications [28]. Cytoplasmic translation (seven proteins) and glycolysis (seven proteins) where the most represented biological processes in the cells growing in either condition. Interestingly, pyruvate decarboxylase 1 (Pdc1), a key enzyme in alcoholic fermentation, and Adh1, the major enzyme responsible for ethanol synthesis, were also found, suggesting a possible role of S-persulfidation in fermentation. The identities of some glycolytic enzymes, glyceraldehyde 3-phosphate dehydrogenase (GAPDH), eno-lase, and triosephosphate isomerase (Tdh3, Eno2, and Tpi1, respectively) were confirmed using specific antibodies (Figure 2). We also tested cystathionine beta-synthase (Cys4), which was described before as a possible S-persulfidated protein [17, 29], although it must be considered that in our mass spectrometry analysis it did not pass the threshold (unused score of 1.04, coverage of 43.98%), we did find that Cys4 was a target of S-persulfidation.

H_2S production during yeast growth

In order to evaluate H_2S production during yeast growth, we determined H_2S in the wt. The H_2S reached a maximal amount during the log phase and dropped its

302 production (Figure 3). Suggesting that the H_2S concentration is not constant and
303 drops when the culture stops growing.

304

305 *H_2S increases glycolytic enzymes activities*

306 Among the first effects of S-persulfidation described was the increase in GAPDH
307 activity [17]. Considering that Tdh3 (GAPDH) was one of the glycolytic enzymes
308 targeted for S-persulfidation, we decided to test the effect of NaHS (a donor of
309 H_2S) on GAPDH activity. Cells were stimulated with 0.1 mM or 0.25 mM NaHS
310 for two and seven hours. Then, the protein was extracted, and the GAPDH activity
311 was measured. We found that after two hours of NaHS stimulation, both at 0.1
312 mM and at 0.25 mM, increased GAPDH activity 1.4 times (Figure 4A), and the
313 effect was lost at seven hours (Figure 4B). Another protein identified by mass
314 spectrometry was pyruvate kinase (PK) that catalyzes the last irreversible step of
315 glycolysis. We measured the activity of the pyruvate kinase at two hours of
316 treatment with 0.1 mM or 0.25 mM NaHS finding that NaHS increased PK activity
317 2.39 times (Figure 4C, Supplementary Table 3), and lost its effect at seven hours
318 (Figure 4D). Finally, we subjected alcohol dehydrogenase (ADH) to the same
319 treatment, and we did not find any significant difference between the treated and
320 untreated cells, i.e., at these concentrations NaHS did not affect ADH activity
321 (Supplemental Figure 1).

322

323 *H_2S stimulates fermentation*

324 The glycolytic enzymes GAPDH and PK increased their activity in response to
325 H2S. In addition, mass spectrometry data indicated that these and other enzymes
326 from gly-colysis were S-persulfidated. Thus, we decided to test whether H_2S
327 influenced the syn-thesis of ethanol. Exponential-phase-grown cells were treated
328 with 0.1 mM NaHS and after seven hours, the supernatant was collected. It was

329 observed that the treated cells had increased ethanol production as compared to
330 the control (Figure 5A).

331 In order to test the effect of endogenous H_2S in fermentation, we decided to
332 compare ethanol production in the two isogenic lab strains BY4741 and BY4742.
333 The only difference between these two strains is that BY4741 has a deletion of
334 *MET17* and strain BY4742 has a deletion of LYS2. As mentioned before, the
335 *met17*Δ strain endogenously accumulates H_2S, because *MET17* codifies for the
336 enzyme using H_2S and O-acetyl homoserine to synthetize homocysteine. An
337 overnight preculture of each strain was diluted to an OD600=0.2, the
338 supernatants were collected after 24 h, and the ethanol was quantified. The strain
339 ac-cumulating H_2S endogenously, BY4741 *met17*Δ, produced more ethanol than
340 the strain BY4742 *MET17* (Figure 5B).

341 Ethanol is the main product of fermentation. Additionally, during glycolytic
342 fermentation two ATP molecules are synthesized. Thus, we decided to quantify
343 the ATP after treatment with NaHS. Exponential-phase cells were treated with
344 the same quantities of NaHS used before, and the ATP was quantified two and
345 four hours after treatment. After two hours, the treated cells produced more ATP
346 than the untreated cells; this effect was lost four hours after treatment (Figure
347 5C). These results suggest that H_2S stimulates glycolysis, and that fermentation
348 is enhanced to produce both ATP and ethanol.

349 Based on these results we decided to compare whether the endogenous H_2S had
350 an influence on the onset of ethanol synthesis. We measured the ethanol
351 production of the poor H_2S producer strain *met5*Δ*met10*Δ, the H_2S accumulator
352 *met17*Δ strain, and the wt. The cells from 48 hours preculture were resuspended
353 in fresh media and aliquots from the supernatant were collected every hour. The
354 *met17*Δ strain initiated ethanol production at five hours, the wt strain initiated
355 production at six hours, and the *met5*Δ*met10*Δ initiated production after seven
356 hours (Figure 6A). This result showed that the cells with high endogenously
357 accumulated H_2S began ethanol production before the cells with a lower H_2S
358 concentration.

Finally, in each of these strains we quantified the ATP at the exponential or stationary phase. We found that the endogenously H_2S accumulator strain produced the most ATP during the exponential phase, while there were no differences in the ATP concentration at the stationary phase between the wt and mutant strains (Figure 6B). These results support our proposal that H_2S stimulates ethanol and ATP production.

Endogenous H_2S accumulation promotes basal oxygen consumption

ATP could be synthesized as product of the glycolysis and the oxidative phosphorylation. In order to elucidate if the ATP produced by H_2S stimulation was from oxidative phosphorylation, we measured oxygen consumption from wt strain and mu-tants. A 48 hours preculture of each strain was diluted to an OD600= 0.2, and oxygen consumption was measured. Then, after seven hours (when cells were at exponential phase) oxygen was measured again (Figure 7). We found, in the diluted cells, that the *met5*Δ*met10*Δ, and the *met17*Δ consumed more oxygen than the *wt* strain. On the other hand, after seven hours of growing, we found that the *met17*Δ strain maintained the el-evated rate of oxygen consumption. This result suggest that endogenously accumulated H_2S promotes oxygen consumption.

H_2S stimulates ethanol production in Meyerozyma guilliermondii and Kluyveromyces marxianus

Ethanol synthesis is more robust in Crabtree positive yeast species; this phenomenon is associated with the WGD [30]. Evidence suggests that the WGD event arose from an interspecies hybridization between a strain from the KLE clade (genera Kluyveromyces, Lachancea and Eremothecium) and a strain from the ZT clade (Zygosaccharomyces and Torulaspora) [31]. The CUG-Ser1 clade

386 first appeared approximately 117 million years before the WGD event; the CUG-
387 Ser1 clade is characterized by a change in codon usage [32]. Considering this,
388 we decided to test the effect of H_2S during ethanol synthesis on the KLE clade
389 strain, *K. marxianus* and in *M. guilliermondii* from the CUG-Ser1 clade. *K.*
390 *marxianus* exponential-phase cells were stimulated with NaHS. Treatment with
391 the H_2S donor in *K. marxianus* increased ethanol synthesis as in *S. cerevisiae*
392 (Figure 8a). In *M. guilliermondii*, it was noted that ethanol synthesis took longer
393 than 24 h when glucose was the carbon source [33]; for this reason, the
394 exponential-phase cells were treated with NaHS and treated again 24 h later. As
395 observed in *K. marxianus*, ethanol synthesis increased after the H_2S donor
396 treatment on *M. guilliermondii* (Figure 8b) confirming that there is an effect of H_2S
397 on the fermentation activity of these two species of yeast.

398

399 **Discussion**

400 Hydrogen sulfide is produced endogenously in yeast, and it is considered a fer-
401 mentation byproduct; however its biological role is unknown. The biological
402 effects of H_2S are linked to a cysteine posttranslational modification termed S-
403 persulfidation [17]. In this work, we analyzed S-persulfidated proteins on the yeast
404 proteome. We identified several glycolytic enzymes as S-persulfidation targets,
405 as reported previously in tissues such as the brain, heart and liver [29], in
406 hepatocytes [17], a pancreatic beta cell line [34], HEK293 cells [29], plant [35,36]
407 and bacteria [37]. Interestingly, Fu and collaborators reported six S-persulfidated
408 glycolytic enzymes (ALDOA, GAPDH, PGK1, ENO1, PKM and LDHA) when they
409 evaluated S-persulfidated proteins in cells overexpressing the H2S-producer
410 enzyme cystathionine gamma-lyase (CSE) [29]. In a previous report, in
411 pancreatic beta cells, metabolites were measured, and H_2S was associated with
412 an increased glycolytic metabolic flux of cells under chronic stress. All these
413 reports agreed that several glycolytic enzymes were S-persulfidated, even when
414 the activity of GAPDH was the only one measured [17]. Cysteine's
415 posttranslational modifications of glycolytic enzymes regulate the subcellular

localization and oligomerization, which can impact its activity [38–40]. In a cell culture, H_2S production is not constant, it starts to decline when the cells are at the middle of the logarithmic phase, suggesting that H_2S synthesis could be regulated by the metabolic conditions. In *S. cerevisiae*, we found that GAPDH increased its activity with the H_2S donor NaHS two hours after the treatment, and the effect was lost at seven hours. It is important to note that H_2S is released from NaHS just a few seconds after the sodium salt is dissolved [41]; hence, the effect of NaHS two hours after treatment may be attributed to a chemical modification of the enzymes, such as S-persulfidation. The thioredoxin system eliminates this posttranslational modification [42,43], which is consistent with the idea that cellular mechanisms maintain protein S-persulfidation homeostasis [44]. Seven hours after stimulation, there was no effect on GAPDH activity probably due to the loss of S-persulfidation by the protein. Furthermore, the cells were no longer at an exponential phase seven hours after the OD600 reached 0.5, and the yeast metabolism changed to aerobic at the diauxic shift. The enzymes catalyzing the irreversible steps regulate the glycolytic pathway [45]; and we found that the enzyme involved in the last irreversible step, pyruvate kinase, increased its activity when stimulated with NaHS. The increase in pyruvate kinase activity may have at least two important consequences: feeding the Krebs cycle and/or stimulating the synthesis of ethanol. Considering that yeast synthe-tizes H_2S during fermentation, we decided to test whether NaHS increased ethanol production. We found that cells treated with the H_2S donor produced more ethanol. In order to confirm our observations, we measured the ethanol production in the isogenic strains BY4741 and BY4742. These strains have almost the same selection markers, and they differ only in one of them, BY4741 accumulates H_2S because it is *met17*Δ; BY4742 is *lys2*Δ, and thus, it does not accumulate H_2S. We observed that BY4741 produced more ethanol than BY4742, suggesting that endogenous H_2S levels increase ethanol synthesis. Previously, it was reported that BY4742 fermenting activity was slower than in BY4741; it would be interesting to analyze the role of H_2S in this system [46]. Considering these results, we proposed that if H_2S stimulates fermentation, then mutants accumulating H_2S would begin ethanol production before strains producing less H_2S. We tested this hy-pothesis by comparing ethanol production between a lower producer of H_2S, the strain *met5*Δ*met10*Δ, the accumulator

strain *met17*Δ, and the *wt*. We found that the *met17*Δ strain started to produce ethanol before the wt strain; in turn, the *met5*Δ*met10*Δ strain production of ethanol was delayed even longer. The results confirmed that endogenous concentrations of H_2S affects ethanol synthesis. Finally, we measured ATP production in all strains, and we found that at the logarithmic phase the *met17*Δ strain produced more ATP than the others. This result supports the idea that in addition to increasing an early synthesis of ethanol, H_2S and also enhances ATP production at the exponential phase of growth.

The fermentation and the oxidative phosphorylation could yield ATP. We found that at exponential phase the *met17*Δ strain produced more ATP than the wt and *met5*Δ*met10*Δ strains. In order to test if the ATP was produced from the oxidative phosphorylation, we measured basal oxygen consumption on these strains. We found that the *met17*Δ strain has an elevated rate of oxygen consumption, and this is sustained when cells were at ex-ponential phase of growth; suggesting that endogenously accumulated H_2S induces oxygen consumption. This would be contradictory to a report where described that ex-ogenous H_2S inhibit respiration [47], however, at physiological concentrations H_2S could induce the S-persulfidation of the ATP synthase from mammals and increases its activity [48]. The S-persulfidation takes place at cysteines 244 and 294 of human ATP synthase. The yeast ATP synthase (Atp1) conserved the cysteine 244 (Supplementary figure 2) in lineal sequence and has similar orientation on protein structure; therefore, the S-persulfidation could also be carried out in Atp1. Our results suggest that endogenous H_2S has an effect on glycolysis and oxygen consumption. The effect of endogenous H_2S on metabolism may explain the advantage of the *met17*Δ strain growing on fermentable carbon sources (glucose and galactose), over the *wt* and *met5*Δ*met10*Δ strains (Supple-mentary figure 3).

It is accepted that the origin of *S. cerevisiae* comes from a WGD event, probably by the interspecies hybridization between a strain from the KLE clade and a strain from the ZT clade [31]. WGD species have a more pronounced Crabtree effect than non-WGD species [30], so we decided to test whether H2S influenced yeast from the parental KLE clade that originated S. cerevisiae and a Crabtree-negative

481 species from the CUG-Ser1 clade. The origin of this clade is estimated to be
482 between 178 and 248 million years ago (mya), and this event occurred before
483 WGD, estimated to be between 82 and 105 mya [32]. We found that both species
484 increase ethanol production after the NaHS treatment suggesting that i) H2S is a
485 positive regulator of fermentation and ii) this effect is evolutionarily conserved.

486 Overall, H2S is considered as a fermentation byproduct on yeast even when its
487 biological effect is unknown. Here, we proposed a very different picture that will
488 change our vision of how H2S regulates cell metabolism.

489

490 **5. Conclusions**

491 In conclusion, our data demonstrated that H_2S is a regulator of energetic
492 metabolism. These results fill a major gap in the understanding of H_2S and its
493 control of ethanol production, which is evolutionarily conserved among yeast
494 species. Finally, our work provides the foundation for a mechanistic
495 understanding of the effects of H_2S.

496 Supplementary Materials: Figure S1: Alcohol dehydrogenase activity; Figure S2:
497 ATP synthase alignment; Figure S3: wt, met5Δmet10Δ, and met17Δ strains
498 growth curves; Table S1: Strains and oligonucleotides primers; Table S2: Mass
499 spectrometry results; Table S3: Protein activity data

500

501 **Funding**

502 This work was supported by the Programa de Apoyo a Proyectos de
503 Investigación e Innovación Tecnológica from the Dirección General de Asuntos
504 del Personal Academico of the Universidad Nacional Autonoma de Mexico (FTQ:

505 UNAM-DGAPA-PAPIIT IA200315, IA202217 and IN209219; SUC: IN208821)
506 and from the Consejo Nacional de Ciencia y Tecnología, Convocatoria de Ciencia
507 Básica to FTQ (CONACyT-CB-238681).

508 **Acknowledgments**

509 Authors acknowledge Dr. Antonio Peña and Dr. Norma Silvia Sanchez for the
510 Kluyveromyces marxianus and Meyerozyma guilliermondii strains provided, Dr.
511 Natalia Chi-quete-Félix, Dr. Gabriel del Rio and Dr. Teresa Lara for technical
512 assistance.

513

514 **References**

515 1. Yang, G.; Wu, L.; Jiang, B.; Yang, W.; Qi, J.; Cao, K.; Meng, Q.; Mustafa,
516 A.K.; Mu, W.; Zhang, S.; et al. H2S as a Physiologic Vasorelaxant: Hypertension
517 in Mice with Deletion of Cystathionine Gamma-Lyase. Science 2008, 322, 587–
518 590, doi:10.1126/science.1162667.

519 2. Kawabata, A.; Ishiki, T.; Nagasawa, K.; Yoshida, S.; Maeda, Y.;
520 Takahashi, T.; Sekiguchi, F.; Wada, T.; Ichida, S.; Nishikawa, H. Hydrogen
521 Sulfide as a Novel Nociceptive Messenger. Pain 2007, 132, 74–81,
522 doi:10.1016/j.pain.2007.01.026.

523 3. Hine, C.; Harputlugil, E.; Zhang, Y.; Ruckenstuhl, C.; Lee, B.C.; Brace, L.;
524 Longchamp, A.; Treviño-Villarreal, J.H.; Mejia, P.; Ozaki, C.K.; et al. Endogenous
525 Hydrogen Sulfide Production Is Essential for Dietary Restriction Benefits. Cell
526 2015, 160, 132–144, doi:10.1016/j.cell.2014.11.048.

527 4. Dooley, F.D.; Nair, S.P.; Ward, P.D. Increased Growth and Germination
528 Success in Plants Following Hydrogen Sulfide Administration. PLoS One 2013,
529 8, e62048, doi:10.1371/journal.pone.0062048.

530 5. Shatalin, K.; Shatalina, E.; Mironov, A.; Nudler, E. H2S: A Universal
531 Defense against Antibiotics in Bacteria. Science 2011, 334, 986–990,
532 doi:10.1126/science.1209855.

533 6. Jiranek, V.; Langridge, P.; Henschke, P.A. Regulation of Hydrogen Sulfide
534 Liberation in Wine-Producing Saccharomyces Cerevisiae Strains by Assimilable
535 Nitrogen. Appl Environ Microbiol 1995, 61, 461–467, doi:10.1128/aem.61.2.461-
536 467.1995.

537 7. Huang, C.-W.; Walker, M.E.; Fedrizzi, B.; Gardner, R.C.; Jiranek, V.
538 Hydrogen Sulfide and Its Roles in Saccharomyces Cerevisiae in a Winemaking
539 Context. FEMS Yeast Res 2017, 17, doi:10.1093/femsyr/fox058.

540 8. Huang, C.; Roncoroni, M.; Gardner, R.C. MET2 Affects Production of
541 Hydrogen Sulfide during Wine Fermentation. Appl Microbiol Biotechnol 2014, 98,
542 7125–7135, doi:10.1007/s00253-014-5789-1.

543 9. Boudreau, T.F.; Peck, G.M.; O'Keefe, S.F.; Stewart, A.C. The Interactive
544 Effect of Fungicide Residues and Yeast As-similable Nitrogen on Fermentation
545 Kinetics and Hydrogen Sulfide Production during Cider Fermentation. J Sci Food
546 Agric 2017, 97, 693–704, doi:10.1002/jsfa.8096.

547 10. Wang, C.; Liu, M.; Li, Y.; Zhang, Y.; Yao, M.; Qin, Y.; Liu, Y. Hydrogen
548 Sulfide Synthesis in Native Saccharomyces Cerevisiae Strains during Alcoholic
549 Fermentations. Food Microbiol 2018, 70, 206–213,
550 doi:10.1016/j.fm.2017.10.006.

551 11. Sun, G.L.; Reynolds, Erin.E.; Belcher, A.M. Using Yeast to Sustainably
552 Remediate and Extract Heavy Metals from Waste Waters. Nat Sustain 2020, 3,
553 303–311, doi:10.1038/s41893-020-0478-9.

554 12. Sohn, H.Y.; Murray, D.B.; Kuriyama, H. Ultradian Oscillation of
555 Saccharomyces Cerevisiae during Aerobic Continuous Culture: Hydrogen
556 Sulphide Mediates Population Synchrony. Yeast 2000, 16, 1185–1190,
557 doi:10.1002/1097-0061(20000930)16:13<1185::AID-YEA619>3.0.CO;2-W.

558 13. Mendoza-Cózatl, D.; Loza-Tavera, H.; Hernández-Navarro, A.; Moreno-
559 Sánchez, R. Sulfur Assimilation and Glutathione Metabolism under Cadmium
560 Stress in Yeast, Protists and Plants. FEMS Microbiol Rev 2005, 29, 653–671,
561 doi:10.1016/j.femsre.2004.09.004.

562 14. Oka, K.; Hayashi, T.; Matsumoto, N.; Yanase, H. Decrease in Hydrogen
563 Sulfide Content during the Final Stage of Beer Fermentation Due to Involvement
564 of Yeast and Not Carbon Dioxide Gas Purging. J Biosci Bioeng 2008, 106, 253–
565 257, doi:10.1263/jbb.106.253.

566 15. Huang, C.-W.; Walker, M.E.; Fedrizzi, B.; Roncoroni, M.; Gardner, R.C.;
567 Jiranek, V. The Yeast TUM1 Affects Pro-duction of Hydrogen Sulfide from
568 Cysteine Treatment during Fermentation. FEMS Yeast Res 2016, 16, fow100,
569 doi:10.1093/femsyr/fow100.

570 16. D'Andrea, R.; Surdin-Kerjan, Y.; Pure, G.; Cherest, H. Molecular Genetics
571 of Met 17 and Met 25 Mutants of Saccharomyces Cerevisiae: Intragenic
572 Complementation between Mutations of a Single Structural Gene. Mol Gen
573 Genet 1987, 207, 165–170, doi:10.1007/BF00331505.

574 17. Mustafa, A.K.; Gadalla, M.M.; Sen, N.; Kim, S.; Mu, W.; Gazi, S.K.; Barrow,
575 R.K.; Yang, G.; Wang, R.; Snyder, S.H. H2S Signals through Protein S-
576 Sulfhydration. Sci Signal 2009, 2, ra72, doi:10.1126/scisignal.2000464.

577 18. Krishnan, N.; Fu, C.; Pappin, D.J.; Tonks, N.K. H2S-Induced Sulfhydration
578 of the Phosphatase PTP1B and Its Role in the Endoplasmic Reticulum Stress
579 Response. Sci Signal 2011, 4, ra86, doi:10.1126/scisignal.2002329.

580 19. Estrada-Ávila, A.K.; González-Hernández, J.C.; Calahorra, M.; Sánchez,
581 N.S.; Peña, A. Xylose and Yeasts: A Story beyond Xylitol Production. Biochim
582 Biophys Acta Gen Subj 2022, 1866, 130154, doi:10.1016/j.bbagen.2022.130154.

583 20. Bergkessel, M.; Guthrie, C.; Abelson, J. Yeast-Gene Replacement Using
584 PCR Products. Methods Enzymol 2013, 533, 43–55, doi:10.1016/B978-0-12-
585 420067-8.00005-2.

586 21. Paul, B.D.; Snyder, S.H. Protein Sulfhydration. Methods Enzymol 2015,
587 555, 79–90, doi:10.1016/bs.mie.2014.11.021.

588 22. Cost, G.J.; Boeke, J.D. A Useful Colony Colour Phenotype Associated with
589 the Yeast Selectable/Counter-Selectable Marker MET15. Yeast 1996, 12, 939–
590 941, doi:10.1002/(SICI)1097-0061(199608)12:10%3C939::AID-
591 YEA988%3E3.0.CO;2-L.

592 23. Choi, K.-M.; Kim, S.; Kim, S.; Lee, H.M.; Kaya, A.; Chun, B.-H.; Lee, Y.K.;
593 Park, T.-S.; Lee, C.-K.; Eyun, S.-I.; et al. Sulfate Assimilation Regulates Hydrogen
594 Sulfide Production Independent of Lifespan and Reactive Oxygen Species under
595 Methionine Restriction Condition in Yeast. Aging (Albany NY) 2019, 11, 4254–
596 4273, doi:10.18632/aging.102050.

597 24. Peña, A.; Sánchez, N.S.; González-López, O.; Calahorra, M. Mechanisms
598 Involved in the Inhibition of Glycolysis by Cyanide and Antimycin A in Candida
599 Albicans and Its Reversal by Hydrogen Peroxide. A Common Feature in Candida
600 Species. FEMS Yeast Res 2015, 15, fov083, doi:10.1093/femsyr/fov083.

601 25. Sakai, H.; Suzuki, K.; Imahori, K. Purification and Properties of Pyruvate
602 Kinase from Bacillus Stearothermophilus. J Biochem 1986, 99, 1157–1167,
603 doi:10.1093/oxfordjournals.jbchem.a135579.

604 26. Bergmeyer, H.V.; Gawhn, K.; Grassel, M. Alcohol Dehydrogenase. In
605 Methods of Enzymatic Analysis; Academic Press: New York, 1974; Vol. 1, pp.
606 428–429.

607 27. Marino, S.M.; Li, Y.; Fomenko, D.E.; Agisheva, N.; Cerny, R.L.; Gladyshev,
608 V.N. Characterization of Surface-Exposed Reactive Cysteine Residues in
609 Saccharomyces Cerevisiae. Biochemistry 2010, 49, 7709–7721,
610 doi:10.1021/bi100677a.

611 28. Alcock, L.J.; Perkins, M.V.; Chalker, J.M. Chemical Methods for Mapping
612 Cysteine Oxidation. Chem Soc Rev 2018, 47, 231–268,
613 doi:10.1039/c7cs00607a.

614 29. Fu, L.; Liu, K.; He, J.; Tian, C.; Yu, X.; Yang, J. Direct Proteomic Mapping
615 of Cysteine Persulfidation. Antioxid Redox Signal 2020, 33, 1061–1076,
616 doi:10.1089/ars.2019.7777.

617 30. Dashko, S.; Zhou, N.; Compagno, C.; Piškur, J. Why, When, and How Did
618 Yeast Evolve Alcoholic Fermentation? FEMS Yeast Res 2014, 14, 826–832,
619 doi:10.1111/1567-1364.12161.

620 31. Marcet-Houben, M.; Gabaldón, T. Beyond the Whole-Genome
621 Duplication: Phylogenetic Evidence for an Ancient In-terspecies Hybridization in
622 the Baker's Yeast Lineage. PLoS Biol 2015, 13, e1002220,
623 doi:10.1371/journal.pbio.1002220.

624 32. Shen, X.-X.; Opulente, D.A.; Kominek, J.; Zhou, X.; Steenwyk, J.L.; Buh,
625 K.V.; Haase, M.A.B.; Wisecaver, J.H.; Wang, M.; Doering, D.T.; et al. Tempo and

626 Mode of Genome Evolution in the Budding Yeast Subphylum. Cell 2018, 175,
627 1533-1545.e20, doi:10.1016/j.cell.2018.10.023.

628 33. Fabricio, M.F.; Valente, P.; Záchia Ayub, M.A. Oleaginous Yeast
629 Meyerozyma Guilliermondii Shows Fermentative Metabolism of Sugars in the
630 Biosynthesis of Ethanol and Converts Raw Glycerol and Cheese Whey Permeate
631 into Polyunsaturated Fatty Acids. Biotechnol Prog 2019, 35, e2895,
632 doi:10.1002/btpr.2895.

633 34. Gao, X.-H.; Krokowski, D.; Guan, B.-J.; Bederman, I.; Majumder, M.;
634 Parisien, M.; Diatchenko, L.; Kabil, O.; Willard, B.; Banerjee, R.; et al. Quantitative
635 H2S-Mediated Protein Sulfhydration Reveals Metabolic Reprogramming during
636 the Integrated Stress Response. Elife 2015, 4, e10067, doi:10.7554/eLife.10067.

637 35. Aroca, Á.; Serna, A.; Gotor, C.; Romero, L.C. S-Sulfhydration: A Cysteine
638 Posttranslational Modification in Plant Systems. Plant Physiol 2015, 168, 334–
639 342, doi:10.1104/pp.15.00009.

640 36. Aroca, A.; Benito, J.M.; Gotor, C.; Romero, L.C. Persulfidation Proteome
641 Reveals the Regulation of Protein Function by Hydrogen Sulfide in Diverse
642 Biological Processes in Arabidopsis. J Exp Bot 2017, 68, 4915–4927,
643 doi:10.1093/jxb/erx294.

644 37. Peng, H.; Zhang, Y.; Palmer, L.D.; Kehl-Fie, T.E.; Skaar, E.P.; Trinidad,
645 J.C.; Giedroc, D.P. Hydrogen Sulfide and Reactive Sulfur Species Impact
646 Proteome S-Sulfhydration and Global Virulence Regulation in Staphylococcus
647 Aureus. ACS Infect Dis 2017, 3, 744–755, doi:10.1021/acsinfecdis.7b00090.

648 38. Aroca, A.; Schneider, M.; Scheibe, R.; Gotor, C.; Romero, L.C. Hydrogen
649 Sulfide Regulates the Cytosolic/Nuclear Partitioning of Glyceraldehyde-3-
650 Phosphate Dehydrogenase by Enhancing Its Nuclear Localization. Plant Cell
651 Physiol 2017, 58, 983–992, doi:10.1093/pcp/pcx056.

652 39. Mitchell, A.R.; Yuan, M.; Morgan, H.P.; McNae, I.W.; Blackburn, E.A.; Le
653 Bihan, T.; Homem, R.A.; Yu, M.; Loake, G.J.; Michels, P.A.; et al. Redox
654 Regulation of Pyruvate Kinase M2 by Cysteine Oxidation and S-Nitrosation.
655 Biochem J 2018, 475, 3275–3291, doi:10.1042/BCJ20180556.

656 40. Ford, A.E.; Denicourt, C.; Morano, K.A. Thiol Stress-Dependent
657 Aggregation of the Glycolytic Enzyme Triose Phosphate Isomerase in Yeast and
658 Human Cells. Mol Biol Cell 2019, 30, 554–565, doi:10.1091/mbc.E18-10-0616.

659 41. Li, L.; Whiteman, M.; Guan, Y.Y.; Neo, K.L.; Cheng, Y.; Lee, S.W.; Zhao,
660 Y.; Baskar, R.; Tan, C.-H.; Moore, P.K. Characterization of a Novel, Water-
661 Soluble Hydrogen Sulfide-Releasing Molecule (GYY4137): New Insights into the
662 Biology of Hydrogen Sulfide. Circulation 2008, 117, 2351–2360,
663 doi:10.1161/CIRCULATIONAHA.107.753467.

664 42. Ju, Y.; Wu, L.; Yang, G. Thioredoxin 1 Regulation of Protein S-
665 Desulfhydration. Biochem Biophys Rep 2016, 5, 27–34,
666 doi:10.1016/j.bbrep.2015.11.012.

667 43. Wedmann, R.; Onderka, C.; Wei, S.; Szijártó, I.A.; Miljkovic, J.L.; Mitrovic,
668 A.; Lange, M.; Savitsky, S.; Yadav, P.K.; Torregrossa, R.; et al. Improved Tag-
669 Switch Method Reveals That Thioredoxin Acts as Depersulfidase and Controls
670 the Intracellular Levels of Protein Persulfidation. Chem Sci 2016, 7, 3414–3426,
671 doi:10.1039/c5sc04818d.

672 44. Paul, B.D.; Filipovic, M.R. Editorial: Molecular Mechanisms of Thiol-Based
673 Redox Homeostasis and Signaling in the Brain. Front Aging Neurosci 2021, 13,
674 771877, doi:10.3389/fnagi.2021.771877.

675 45. Campbell-Burk, S.L.; Shulman, R.G. High-Resolution NMR Studies of
676 Saccharomyces Cerevisiae. Annu Rev Microbiol 1987, 41, 595–616,
677 doi:10.1146/annurev.mi.41.100187.003115.

678 46. Harsch, M.J.; Lee, S.A.; Goddard, M.R.; Gardner, R.C. Optimized
679 Fermentation of Grape Juice by Laboratory Strains of Saccharomyces
680 Cerevisiae. FEMS Yeast Res 2010, 10, 72–82, doi:10.1111/j.1567-
681 1364.2009.00580.x.

682 47. Wang, T.; Yang, Y.; Liu, M.; Liu, H.; Liu, H.; Xia, Y.; Xun, L. Elemental
683 Sulfur Inhibits Yeast Growth via Producing Toxic Sulfide and Causing Disulfide
684 Stress. Antioxidants (Basel) 2022, 11, 576, doi:10.3390/antiox11030576.

685 48. Módis, K.; Ju, Y.; Ahmad, A.; Untereiner, A.A.; Altaany, Z.; Wu, L.; Szabo,
686 C.; Wang, R. S-Sulfhydration of ATP Synthase by Hydrogen Sulfide Stimulates
687 Mitochondrial Bioenergetics. Pharmacol Res 2016, 113, 116–124,
688 doi:10.1016/j.phrs.2016.08.023.

689

690

691

692

693

694

695

696

697

Figure 1. H_2S productivity correlates with S-persulfidated proteins levels. (A) H_2S productivity by *wt*, *met5*Δ*met10*Δ and *met17*Δ. Cells were incubated at 30°C on YPDL plates for 4 days. (B) S-persulfidated proteins in *wt*, *met5*Δ*met10*Δ and *met17*Δ strains. Whole cell extracts from exponential phase cultures were subjected to the modified biotin switch assay with antibody against biotin (α-Biotin Ab) to detect S-persulfidation.

Figure 2. Confirmation of S-persulfidated proteins by streptavidin beads precipitation. A. Whole cell extracts from exponential phase cultures were subject to the modified biotin switch assay, precipitated with streptavidin beads and detected with antibodies specific to each protein; enolase (Eno2), glyceraldehyde 3 phosphate dehydrogenase (Tdh3), cystathionine beta synthase (Cys4) and triose phosphate isomerase (Tpi1). HPDP-B: (N-[6-(biotinamido)hexyl]-3'-(2'-pyridyldithio)propionamide). B. Whole cell extract from exponential phase cultures after modified biotin switch assay was used as input control. (-) line shows the proteins that reacts with anti-biotin antibody. (+) line shows biotinylated proteins after modified biotin switch assay. TCL: Total cell lysate, PP STREP: Streptavidin precipitation.

Figure 3. H_2S production reach a maximal during log phase. Yeast cell were cultured in 96 wells microplate at 30°C and growth was measured at 600 nm. H_2S was detected measuring methylene blue reduction at 663 nm.

Figure 4. H2S increase the activity of GAPDH and Pyruvate Kinase two hours after stimu-lation. (A) Yeast cell cultures at exponential phase were treated with NaHS 0.1 and 0.25 mM. Two hours later whole cell extracts were used to measure GAPDH activity in vitro at 37°C. One-way ANOVA ** P<0.0001. (B) Yeast cell cultures at exponential phase were treated with NaHS 0.1 and 0.25 mM. Seven hours later whole cell extracts were used to measure GAPDH activity in vitro at 37°C. (C) Yeast cell cultures at exponential phase were treated with NaHS 0.1 and 0.25 mM. Two hours later whole cell extracts were used to measure Pyruvate Kinase activity in vitro at 37°C. (D) Yeast cell cultures at exponential phase were treated with NaHS 0.1 and 0.25 mM. Seven hours later

728 whole cell extracts were used to measure Pyruvate Kinase activity in vitro at
729 37°C. One-way ANOVA * P<0.01. Closed circles, untreated cells; closed squares,
730 NaHS 0.1 mM; closed triangles, NaHS 0.25 .

731 **Figure 5.** Exogenous and endogenous H_2S on yeast cells induce ethanol
732 production and ATP synthesis. (A) BY4742 yeast cell cultures were treated with
733 NaHS 0.1 mM and seven hour later supernatants were collected. Ethanol
734 production was measured in vitro at 37°C. Closed circles, untreated cells; closed
735 squares, NaHS 0.1 mM. Unpaired t * P=0.04. (B) Yeast cell cultures of the strains
736 BY4741 and BY4742 supernatants were collected at 24 h. Ethanol production
737 was measured in vitro at 37°C. Closed squares, BY4741; open squares, BY4742.
738 Unpaired t * P=0.02 (C) Yeast cell cultures at exponential phase were treated
739 with NaHS 0.1 and 0.25 mM. Two and four hours later whole cell extracts were
740 lysated and ATP was quantified. ATP production was measure in vitro at 37°C.
741 Closed circles, untreated cells; closed squares, NaHS 0.1 mM; closed triangles,
742 NaHS 0.25 mM. One-way ANOVA ** P<0.001.

743 **Figure 6.** Yeast mutants that accumulate H_2S synthesize ethanol faster and more
744 ATP than lower endogenously accumulated H_2S. (A) 48 hours precultures of
745 yeast cell of the strains *wt*, *met5*Δ*met10*Δ and *met17*Δ were resuspended in fresh
746 media and supernatants were collected every hour. Ethanol production was
747 measured in vitro at 37°C. (B) Yeast cell cultures at exponential and stationary
748 phase of the strains *wt*, *met5*Δ*met10*Δ and *met17*Δ were lysated and ATP was
749 quantified. ATP production was measure in vitro at 37°C. One-way ANOVA *
750 P<0.05, ** P<0.01. Open circles, *wt*; closed squares, *met5*Δ*met10*Δ; closed
751 diamonds, *met17*Δ.

752 **Figure 7.** Endogenous H_2S promotes basal oxygen consumption. 48 hours
753 precultures of the *wt* and the mutants was diluted to an OD_{600}= 0.2, and oxygen
754 consumption was measured. The basal oxygen consumption was measured in
755 resting cells in a Clark electrode at 30°C. Seven hours after dilution oxygen
756 consumption was measured again. One-way ANOVA * P<0.05, ** P<0.01. Open
757 circles, *wt*; closed squares, *met5*Δ*met10*Δ; closed diamonds, *met17*Δ.

758 **Figure 8.** Exogenous H_2S induce ethanol production in *K. marxianus* and *M.*
759 *guilliermondi*. (A) *K. marxianus* yeast cell cultures were treated with NaHS 0.1
760 mM and seven hour later supernatants were collected. Ethanol production was
761 measured in vitro at 37°C. Unpaired t ** P=0.002. (B) *M. guilliermondi* yeast cell
762 cultures were treated with NaHS 0.1 mM and 24 h later cells were treated again
763 with same concentration of NaHS. Seven hour later supernatants were collected.
764 Ethanol production was measured in vitro at 37°C. Unpaired t * P=0.04. Closed
765 circles, untreated cells; closed squares, NaHS 0.1 mM

766

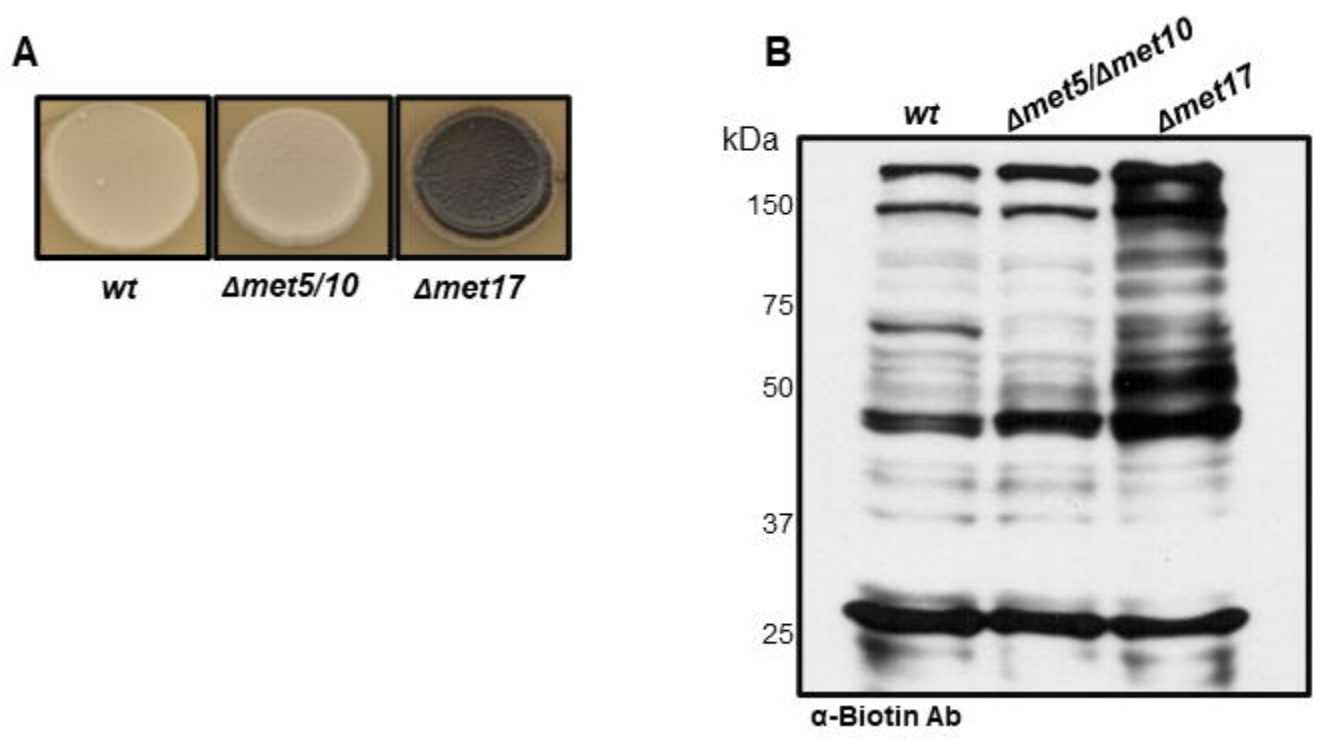
A
wt
Δmet5/10
Δmet17
B
wt
Δmet5/Δmet10
Δmet17
kDa
150
75
50
37
25
α-Biotin Ab

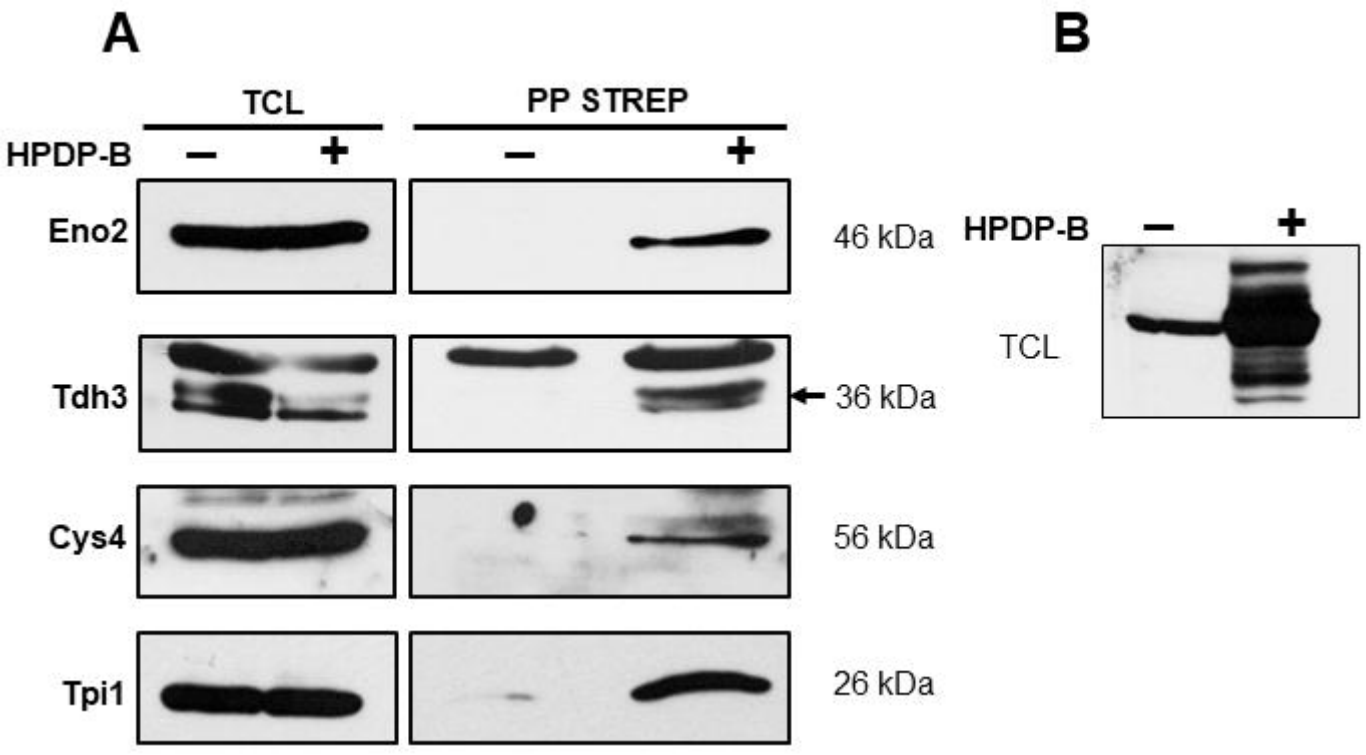
A
TCL
PP STREP
HPDP-B
–
+
–
+
Eno2
46 kDa
Tdh3
36 kDa
Cys4
56 kDa
Tpi1
26 kDa
B
HPDP-B
–
+
TCL

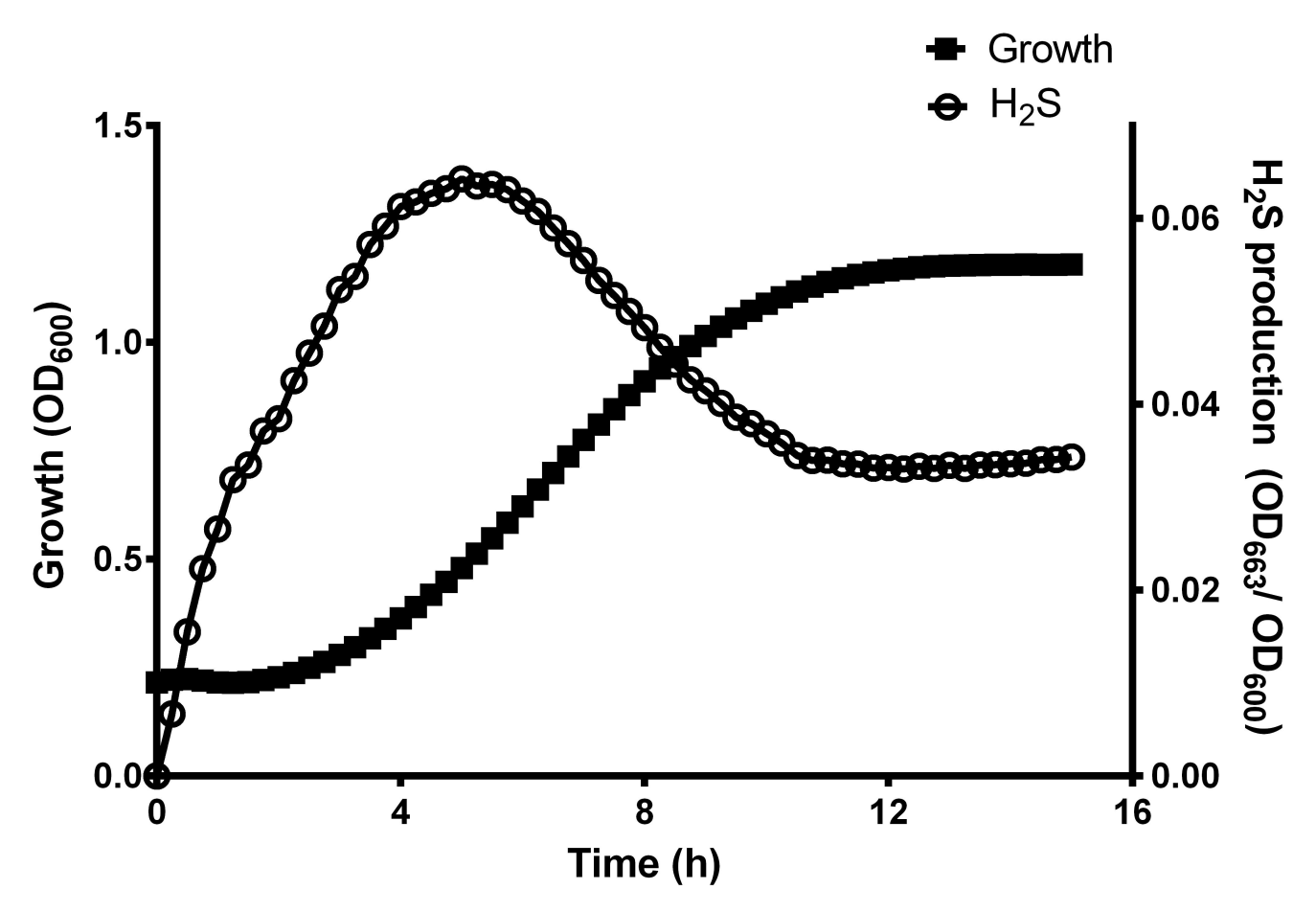
Growth
H2S
1.5
1.0
0.5
0.0
Growth (OD600)
0.06
0.04
0.02
0.00
H2S production (OD663/ OD600)
0
4
8
12
16
Time (h)

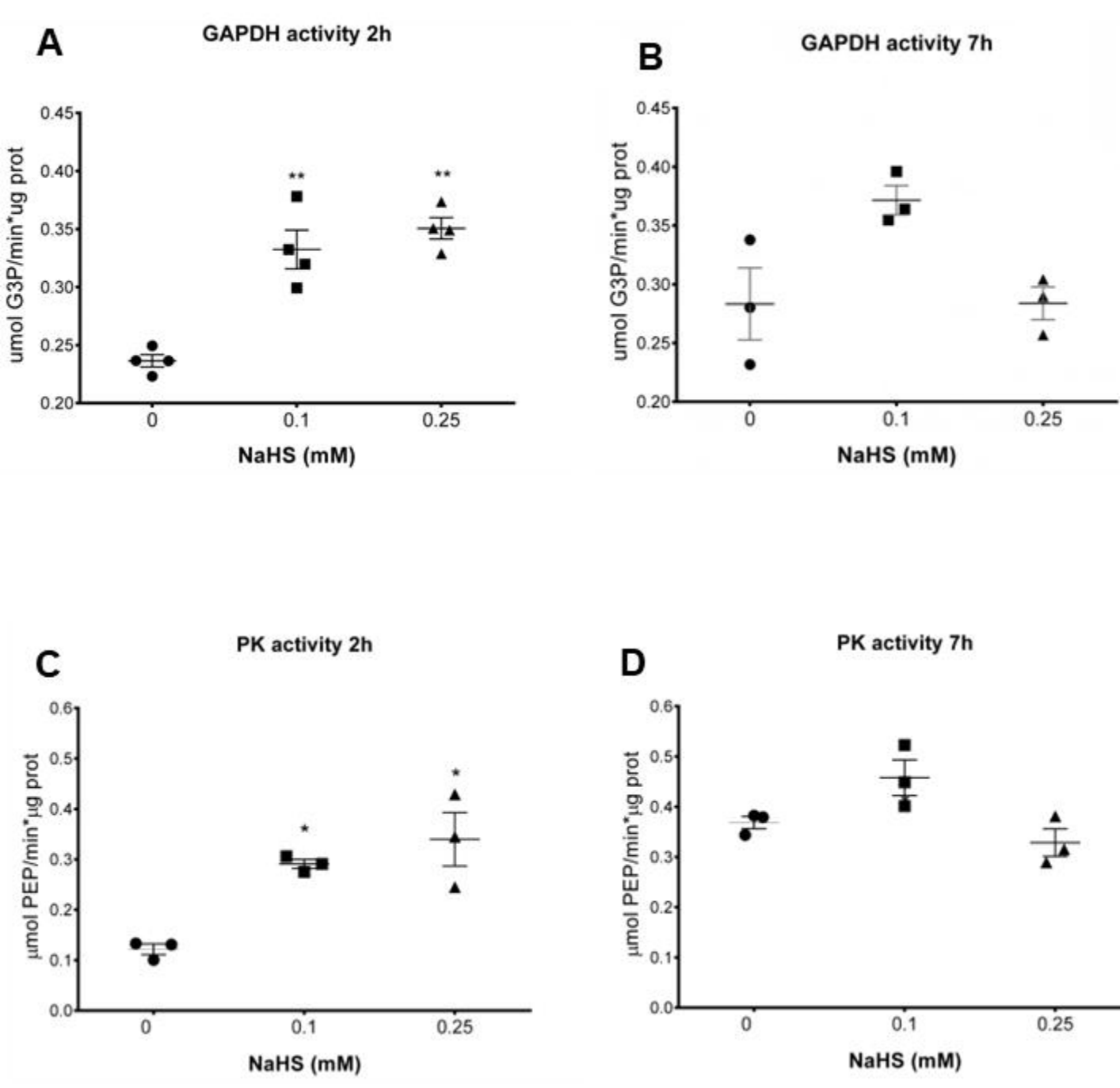
A
GAPDH activity 2h
umol G3P/min*ug prot
0.45
0.40
0.35
0.30
0.25
0.20
**
**
0
0.1
0.25
NaHS (mM)
B
GAPDH activity 7h
umol G3P/min*ug prot
0.45
0.40
0.35
0.30
0.25
0.20
0
0.1
0.25
NaHS (mM)
C
PK activity 2h
µmol PEP/min*µg prot
0.6
0.5
0.4
0.3
0.2
0.1
0.0
*
*
0
0.1
0.25
NaHS (mM)
D
PK activity 7h
µmol PEP/min*µg prot
0.6
0.5
0.4
0.3
0.2
0.1
0.0
0
0.1
0.25
NaHS (mM)

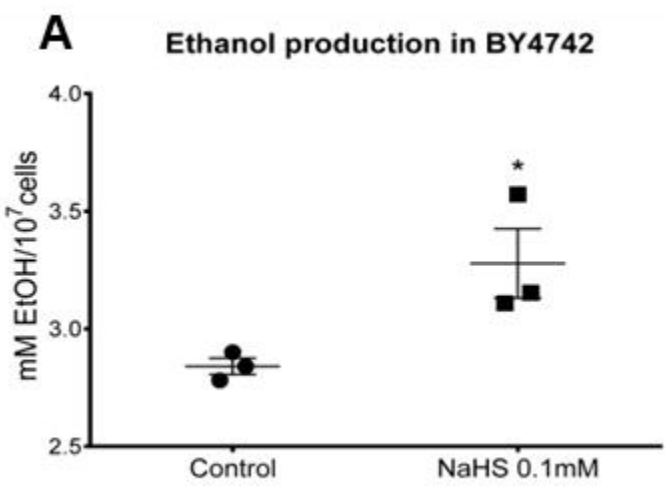
A
Ethanol production in BY4742
mM EtOH/10^7 cells
4.0
3.5
3.0
2.5
*
Control
NaHS 0.1mM

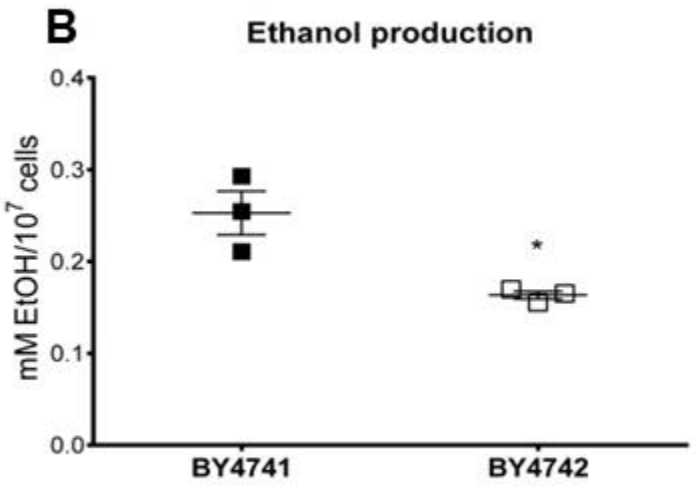
B
Ethanol production
mM EtOH/10^7 cells
0.4
0.3
0.2
0.1
0.0
*
BY4741
BY4742

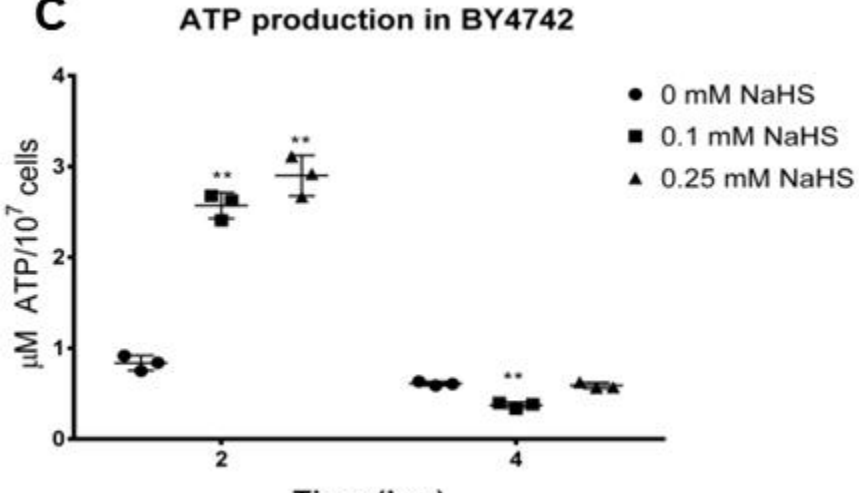
C
ATP production in BY4742
μM ATP/10^7 cells
4
3
2
1
0
**
**
**
2
4
Time (hrs)
0 mM NaHS
0.1 mM NaHS
0.25 mM NaHS

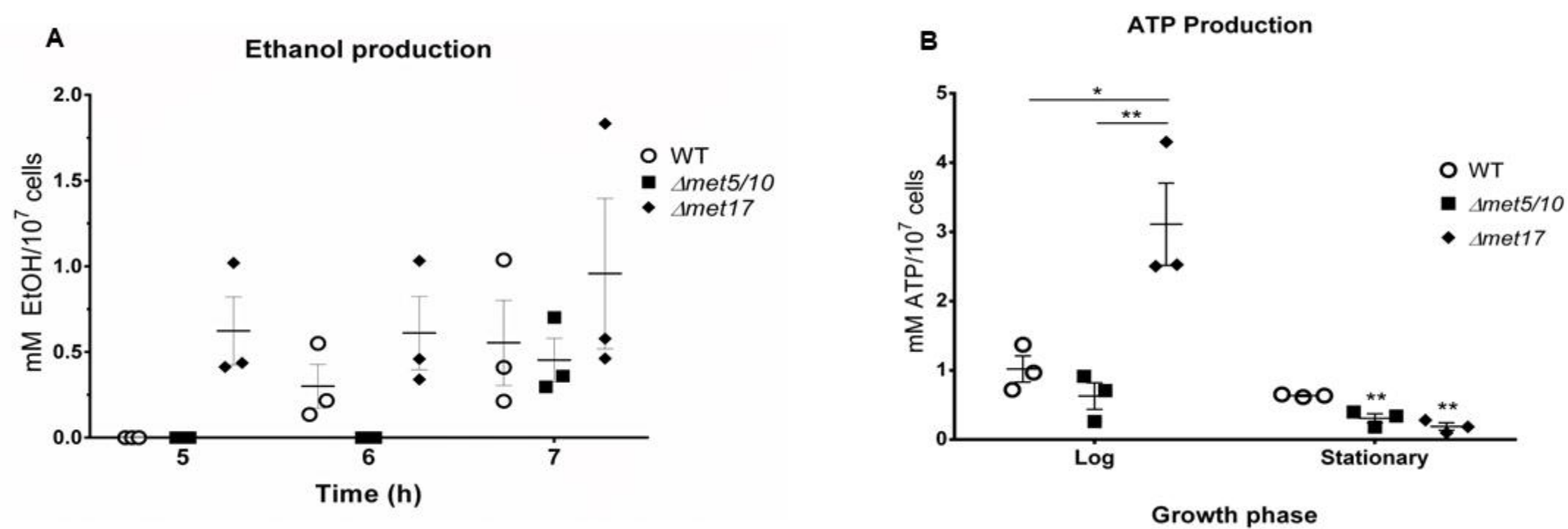
A
Ethanol production
mM EtOH/10^7 cells
2.0
1.5
1.0
0.5
0.0
5
6
7
Time (h)
WT
Δmet5/10
Δmet17
B
ATP Production
mM ATP/10^7 cells
5
4
3
2
1
0
*
**
**
**
Log
Stationary
Growth phase
WT
Δmet5/10
Δmet17

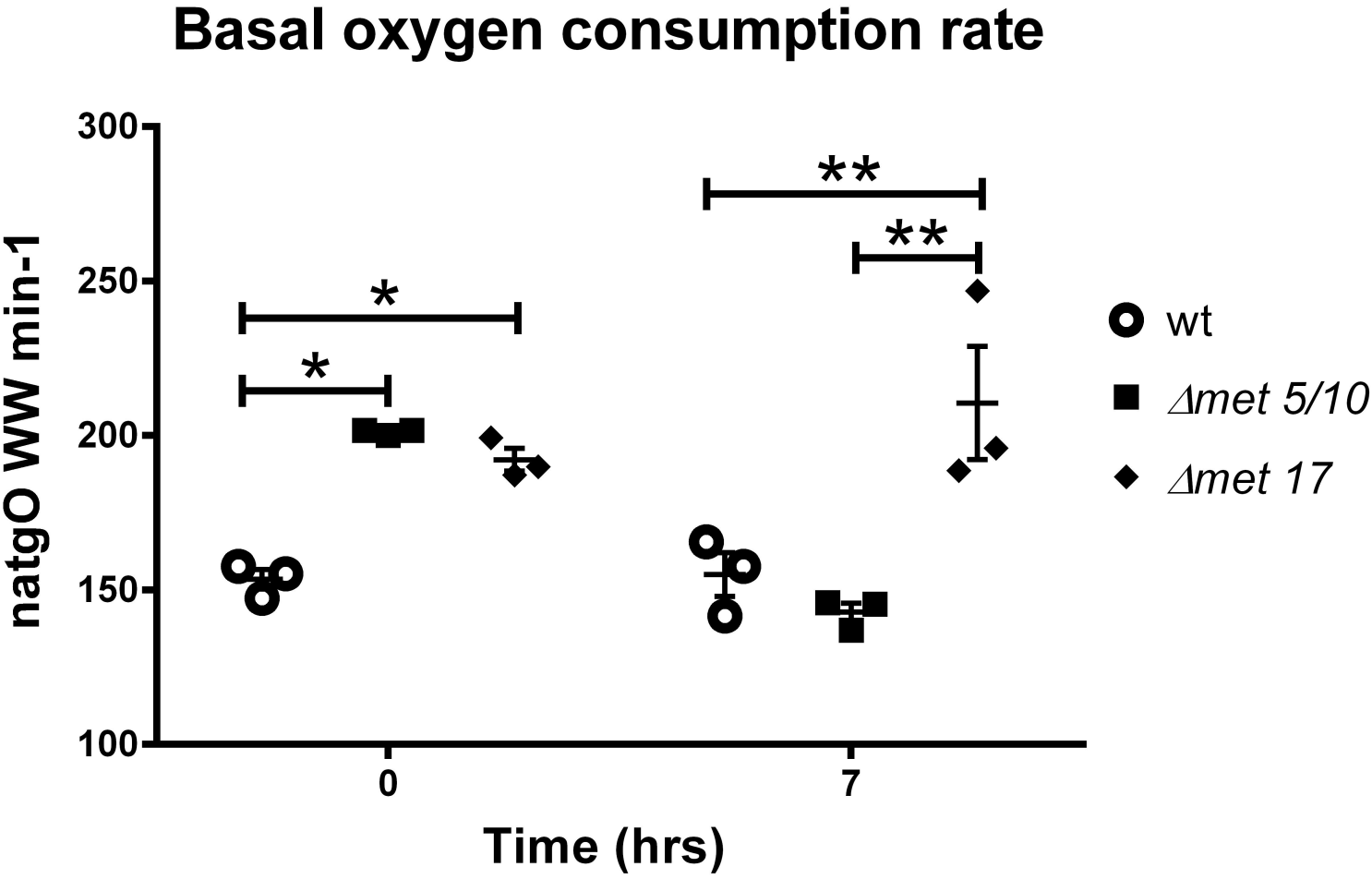
Basal oxygen consumption rate
300
250
200
150
100
natgO WW min-1
*
*
**
**
0
7
Time (hrs)
wt
Δmet 5/10
Δmet 17

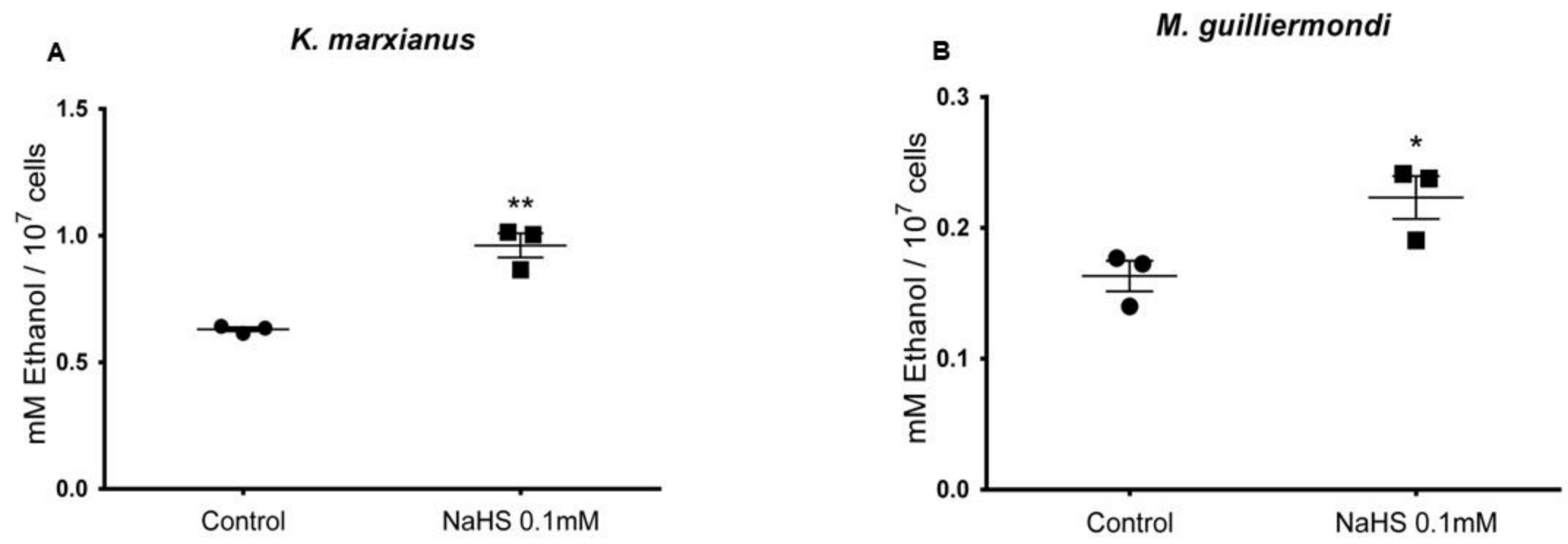
A
K. marxianus
mM Ethanol / 10^7 cells
1.5
1.0
0.5
0.0
**
Control
NaHS 0.1mM
B
M. guilliermondi
mM Ethanol / 10^7 cells
0.3
0.2
0.1
0.0
*
Control
NaHS 0.1mM